Modeling of Hydrogen Jet Diffusion Flames*
(On the Direct Influence of Molecular Viscosity)

Yoshiaki ONUMA**, Noriyoshi MORINAGA**,
Yoshiki MORINAGA** and Kaoru FURUSHIMA**

It was believed that the increase of molecular viscosity due to high temperature raises the dissipation rate of turbulence in low-turbulent regions in a combustion field. Hence, the objective of the present study was to verify this both experimentally and theoretically. Experiments were carried out on jet diffusion flames of hydrogen, and then, a numerical simulation was conducted for the experimental results. In the simulation, the k-ε two-equation model was used as a turbulence model and a new source term was added to the k-equation to represent the dissipation rate of turbulence kinetic energy due to molecular viscosity. The calculated results agreed well with the experimental ones. It was found that the new source term suppresses turbulence in low turbulent regions situated around the nozzle exit and the periphery of jets, and changes the condition in the whole combustion field greatly. The present work suggested that consideration of the viscous effect is important in the modeling of turbulent combustion fields.

Key Words: Combustion, Turbulent Diffusion Flame, Modeling, Turbulence Model, Molecular Viscosity

1. Introduction

Molecular viscosity does not have a direct influence on the dissipation rate of turbulence kinetic energy in regions where the turbulence Reynolds number is sufficiently large. This is because the energy transfer between turbulence eddies caused by inertial force controls the dissipation rate. However, it is well known that the viscous effect is significant in low-Reynolds-number regions. Especially, the direct influence of molecular viscosity has an important role in the phenomena relating to the wall boundary layer, and its modeling has been attempted by many researchers[1]~[6].

Intense turbulence is observed around the nozzle exit in gas jets issuing from a circular nozzle, but the turbulence is extremely suppressed in jet diffusion flames. This phenomenon has been understood as the laminarization due to the existence of flames[7]~[10]. Recently, Takagi et al.[11][12] examined this phenomenon experimentally and attempted the simulation by modifying one of the empirical constants appearing in the k-ε turbulence model. It may be considered that the laminarization is due to the foregoing direct influence of molecular viscosity in low-Reynolds-number regions. Namely, around the nozzle exit where turbulence has not yet developed, the increase of viscosity due to high temperature may raise the dissipation rate of turbulence. Only this phenomenon around the nozzle exit has been recognized as an example of laminarization in combustion fields. However, the regions of high temperature and low turbulence may exist all around the periphery, even downstream, in jet diffusion flames. If these suppositions are correct, the direct influence of molecular viscosity on turbulence field might be a factor greatly controlling the flame structure.

In the present study, to examine these suppositions, experiments were carried out on jet diffusion flames of hydrogen/nitrogen mixtures, and then a numerical simulation was conducted on the flames. The direct influence of viscosity was taken into consideration in the turbulence model, referring to the

* Received 24th August, 1987. Paper No. 87-0213 A
** Department of Energy Engineering, Toyohashi University of Technology, 1-1 Hibarigaoka, Tempaku-cho, Toyohashi, 440, Japan

model proposed by Jones and Launder[1] in the calculation of near-wall flows. The influence that the consideration of the viscous effect brings on the simulation were examined by comparing the calculated results with the experimental ones, and the change of flame structure caused by the laminarization due to flame existence was discussed.

Nomenclature

B : empirical constant appearing in combustion model
c_f : time-averaged fuel concentration
c_0 : time-averaged oxygen concentration
c_1, c_2, c_μ, c_m : empirical constants appearing in the k-ε turbulence model
k : turbulence kinetic energy
l : length scale of turbulence
m : stoichiometric mass ratio of fuel to oxygen
R : turbulent Reynolds number
R_f : reaction rate of fuel
r : radial distance from the axis of symmetry
u : velocity in the stream-wise direction
u' : rms fluctuating velocity
v : velocity in the cross-stream direction
x : distance in the stream-wise direction
ε : dissipation rate of turbulent kinetic energy
ν : kinematic viscosity
ν_{eff} : effective kinematic viscosity
ν_t : turbulent kinematic viscosity
σ_k, σ_ε : turbulent Prandtl number

2. Experiments

2.1 Apparatus and procedure

A turbulent diffusion flame was formed with a fuel gas jet issuing vertically upward from a circular nozzle. A mixture of hydrogen and nitrogen was used as fuel. Inside diameters of the fuel nozzles were 4 mm and 10 mm in the following Experiments 1 and 2, respectively. Surrounding air issues parallel to the fuel jet from a coaxial orifice of 130 mm inside diameter. Time-averaged and rms fluctuating velocities, chemical species concentrations and temperature were measured with a laser doppler velocimeter, gas chromatogragher and thermocouple, respectively.

Table 1 Flow rate of nozzle fluid

Mixing Ratio	Flow Rate (cm^3/s)	
H_2 : N_2	H_2	N_2
1 : 2	114	228
1 : 3	86	257

2.2 Experiment 1: results and discussion

Measurements were carried out on two flames and one cold jet. The mixing ratios of hydrogen to nitrogen in the nozzle fluids were 1 : 2 and 1 : 3 in the two flames respectively, referred to as Flame 1/2 and Flame 1/3 hereafter. The mixing ratio in the cold jet was 1 : 2, hence the name Cold Jet 1/2. Flow rates of hydrogen and nitrogen in the nozzle fluids are shown in Table 1. For all cases, the nominal velocity of nozzle fluid at the nozzle exit was 27.2 m/s and the flow velocity of the surrounding air was 3 m/s.

Figure 1 shows the axial profiles of time-averaged velocity $\bar{U}$ and rms fluctuating velocity u' for the two flames and the cold jet. Here, x is the distance from the nozzle tip and D is the inside diameter of the nozzle. Comparing Flame 1/2 and Cold Jet 1/2, it was found that combustion reduces the decreasing rate of flow velocity on the axis of symmetry ; hence, a high velocity is maintained even downstream in the flame. In rms fluctuating velocity profiles, though the cold jet makes a sharp peak near the nozzle exit and u' dissipates its value rapidly and monotonically after the peak, the flame makes two humps ; the main hump is located much more downstream than that of the cold jet's, and the turbulence just after the nozzle exit is greatly suppressed by the existence of flame.

Figures 2 (a) and (b) show the radial profiles of $\bar{U}$ and u' on the cross sections of $x/D=10$ and 30 in Flame 1/2, respectively. Figures 3 and 4 show the axial and radial profiles of temperature $\bar{T}$ and chemical species concentrations. Plotted temperature are not corrected for thermal radiation loss. These measured results will be compared with the calculated results in the following section.

2.3 Experiment 2: results and discussion

Experiment 1 indicated that the flow field around the nozzle exit is greatly changed by the existence of a flame. To examine this phenomenon more closely,

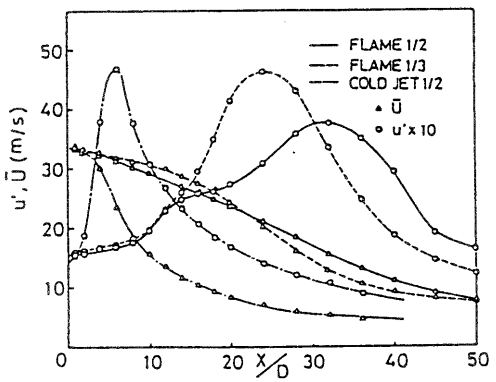

Fig. 1 Axial profiles of time-averaged velocity and rms fluctuating velocity along symmetry axis

the second experiment was conducted with a large fuel nozzle of 10 mm inside diameter. A H_2/N_2 mixture of mixing ratio 1 : 2 was used as fuel. The flow rates of H_2 and N_2 were 500 cm^3/s and 1000 cm^3/s, respectively.

Figure 5 shows the axial profiles of $\bar{U}$, u' and $\bar{T}$ along the axis of symmetry in the jets with and without combustion. It is found that the existence of a flame results in a lengthening of the potential core.

Figures 6 and 7 show the radial profiles on $x/D=3.5$ cross section just after the nozzle exit and on $x/D=12$ cross section after the disappearance of the potential core. In Fig. 6, the turbulence in the flame indicates lower values throughout the cross section compared to that in the cold jet. The turbulence around the peak point of the temperature profile, where the main combustion region is supposed to exist, is extremely small. These phenomena may be attributed to the direct influence of molecular viscosity, as mentioned in the introduction. Namely, the increase of viscosity due to the temperature rise accompanying combustion may in turn raise the dissipation rate of turbulence just after the nozzle exit, where turbulence is first generated and is, thus, still weak. In contrast to these phenomena, it is noted in Fig. 7 that the maximum value of u' is larger in the flame than in the cold jet and the peak point of u' situates around the main combustion region. This is translated to mean that, where the turbulence is sufficiently large, the increase of viscosity due to temperature rise has little effect on turbulence behavior. The first hump of u' appearing upstream in Fig. 1 may be formed relating to these phenomena.

3. Numerical Simulation

3.1 Modeling and calculation

The governing equations consist of the conservation equations of mass, momentum, energy and chemical species, to which boundary layer approximation was applied. The k-ε two-equation model was used as a turbulence model. Usually in this model, turbulence

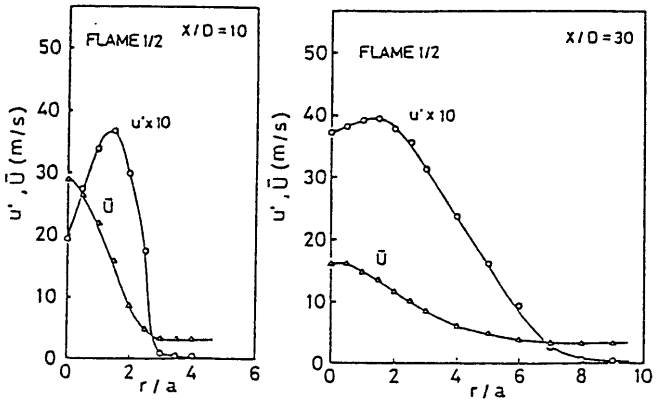

(a) The cross section of $x/D=10$ (b) The cross section of $x/D=30$

Fig. 2 Radial profiles of time-averaged velocity and rms fluctuating velocity on cross section

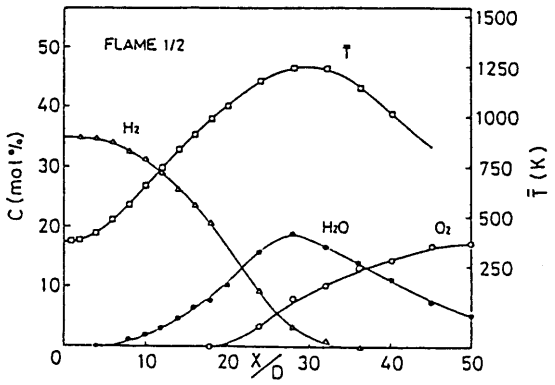

Fig. 3 Axial profiles of temperature and concentrations along symmetry axis for Flame 1/2

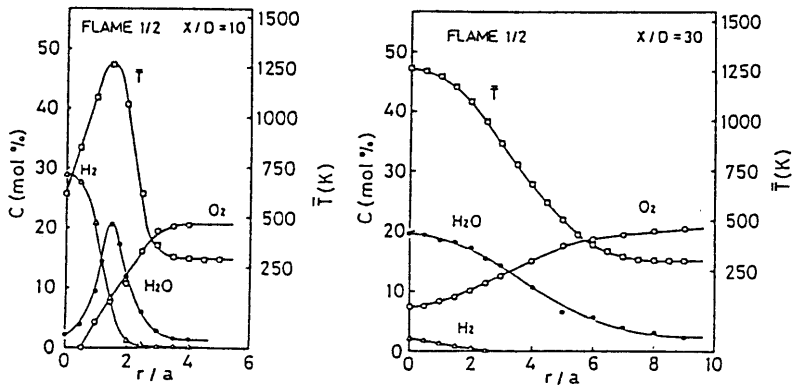

(a) The cross section of $x/D=10$ (b) The cross section of $x/D=30$

Fig. 4 Radial profiles of temperature and concentrations on cross section

kinetic energy k and its dissipation rate ε is obtained from Eqs. (1) and (2), and turbulence kinematic viscosity ν_t from Eq.(3).

$$u\frac{\partial k}{\partial x}+v\frac{\partial k}{\partial r}=\frac{1}{r}\frac{\partial}{\partial r}\left(r\frac{\nu_t}{\sigma_k}\frac{\partial k}{\partial r}\right)+\nu_t\left(\frac{\partial u}{\partial r}\right)^2-\varepsilon \quad (1)$$

$$u\frac{\partial \varepsilon}{\partial x}+v\frac{\partial \varepsilon}{\partial r}=\frac{1}{r}\frac{\partial}{\partial r}\left(r\frac{\nu_t}{\sigma_\varepsilon}\frac{\partial \varepsilon}{\partial r}\right)+c_1\frac{\varepsilon}{k}\nu_t\left(\frac{\partial u}{\partial r}\right)^2-c_2\frac{\varepsilon^2}{k} \quad (2)$$

$$\nu_t=c_\mu k^2/\varepsilon \quad (3)$$

However, Eqs. (1) and (2) can be applied to high-Reynolds-number flow fields, but not those of low Reynolds numbers where molecular viscosity directly influences k and ε.

The foregoing experiments of H_2/N_2 jet diffusion flames suggested that the direct influence of molecular viscosity cannot be neglected around the nozzle exit where turbulence is small and temperature is high. Therefore, considering the direct influence of viscosity, Eqs. (4)~(6) were used instead of Eqs. (1) and (2) in the present study.

$$u\frac{\partial k}{\partial x}+v\frac{\partial k}{\partial r}=\frac{1}{r}\frac{\partial}{\partial r}\left(r\frac{\nu_{eff}}{\sigma_k}\frac{\partial k}{\partial r}\right)+\nu_t\left(\frac{\partial u}{\partial r}\right)^2-\varepsilon-c_m\nu\left(\frac{\partial\sqrt{k}}{\partial r}\right)^2 \quad (4)$$

$$u\frac{\partial \varepsilon}{\partial x}+v\frac{\partial \varepsilon}{\partial r}=\frac{1}{r}\frac{\partial}{\partial r}\left(r\frac{\nu_{eff}}{\sigma_\varepsilon}\frac{\partial \varepsilon}{\partial r}\right)+c_1\frac{\varepsilon}{k}\nu_t\left(\frac{\partial u}{\partial r}\right)^2-c_2\frac{\varepsilon^2}{k} \quad (5)$$

$$\nu_{eff}=\nu_t+\nu \quad (6)$$

The last term in the right-hand side of Eq.(4) represents the dissipation of turbulence controlled by molecular viscosity. The form of this term was decided by referring to the turbulence model of Jones and Launder[1][2] for the study of near-wall flows. The diffusion coefficients of k and ε are $(\nu_t+\nu)/\sigma$ in Eqs. (4) and (5), though they should theoretically be $\nu+\nu_t/\sigma$. This selection is based on the empirical knowledge that it enables the use of the universal values as the five empirical constants (c_μ, c_1, c_2, σ_k, σ_ε) of the k-ε model in the present modified model.

The eddy-dissipation model[13], represented by Eq. (7), was used as a combustion model.

$$\left.\begin{aligned}R_f&=-Bc_f(\varepsilon/k)[c_f\leqq mc_0]\\R_f&=-Bmc_0(\varepsilon/k),\ [c_f>mc_0]\end{aligned}\right\} \quad (7)$$

The condition in developed pipe flow was given to the initial flow condition at the nozzle exit. Namely, the universal velocity distribution was used for flow velocity, mixing length was obtained from Nikuradse's empirical formula, and turbulent kinetic energy was calculated from Eq.(8).

$$k=\left(c_k l\left|\frac{\partial u}{\partial r}\right|\right)^2+k_0 \quad (8)$$

Measured value was used as the turbulent kinetic

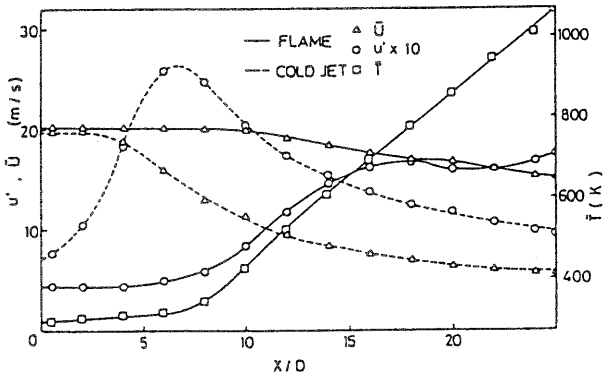

Fig. 5 Axial profiles along symmetry axis (fuel nozzle of large inside diameter)

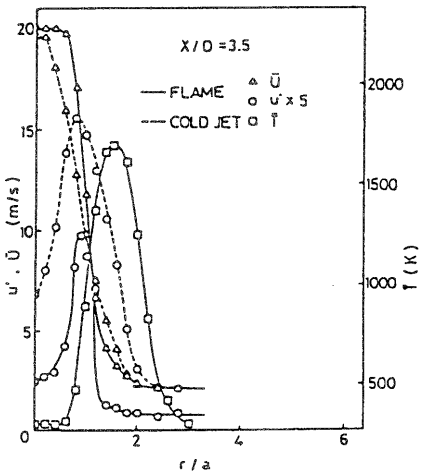

Fig. 6 Radial profiles on the cross section of $x/D=3.5$ (fuel nozzle of large inside diameter)

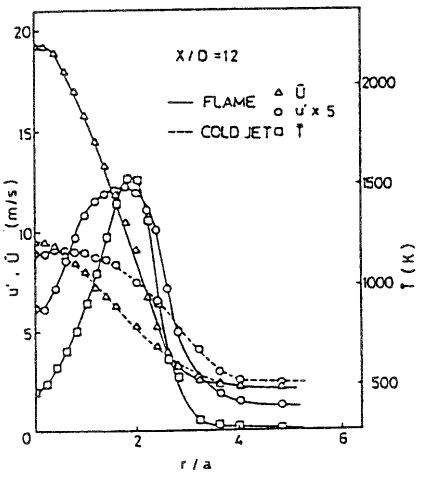

Fig. 7 Radial profiles on the cross section of $x/D=12$ (fuel nozzle of large inside diameter)

energy at the center , k_0. The constant c_k was decided such that the maximum value of k is four times that of k_0, referring to the experimental result reported by Laufer[14].

The GENMIX 4 program[15] was applied to the numerical calculation. For the constants, c_m in Eq. (4) and B in Eq. (7), 2.75 and 2.0 were respectively selected. The other empirical constants were assigned the following values.

$$\left.\begin{aligned} &c_\mu=0.09,\ c_1=1.4,\ c_2=2.0 \\ &\sigma_k=1.0,\ \sigma_\varepsilon=1.3 \end{aligned}\right\} \qquad (9)$$

3.2 Calculated results and discussion

Calculations were conducted on the results of Experiment 1 shown in Figs. 1~4. Figure 8 gives the axial profiles of $\bar{U}$ and k corresponding to the experimental results shown in Fig. 1. The calculated results well represent the experimental ones. It appears that the phenomena in which the existence of flames suppresses the turbulence around the nozzle exit and shifts the peak of turbulence downstream can be described by the present model, at least. qualitatively speaking. The calculated results also reasonably represent the mutual relation among the u' profiles of Cold Jet 1/2, Flame 1/2 and Flame 1/3. An interesting point is that the first hump of u' in the upstream region appears also in the calculated result for Flame 1/2, though incompletely. Because the turbulence is adequately represented, the calculated results for time-averaged velocity $\bar{U}$ coincides with the experimental ones qualitatively and quantitatively.

Figure 9 gives the calculated axial profiles of $\bar{U}$ and k for Cold Jet 1/2. The notations of MVT=1 (solid line) and MVT=0 (broken line) denote the results calculated with and without the last term of Eq. (4), respectively. It is found from this figure that the new dissipation term of molecular viscosity has little effect on calculated results in a noncombustion jet. In contrast, including the new term brings about large change in the calculated results for flames, as shown later in Figs. 10~13.

Figure 10 shows the axial profiles of $\bar{U}$ and k for Flame 1/2. It is noted from Figs. 8 and 10 that, though the peak point of k appears more downstream in the flame than in the cold jet even without taking the new dissipation term into account, its inclusion shifts the peak even more downstream and improves the simulation greatly. Figure 10 indicates that the first hump in the k profile appears with the inclusion of the new term. The effect of the new dissipation term may vary greatly with the large changes of temperature and turbulence around the nozzle exit; this may explain the formation of the first hump.

Figures 11 (a) and (b) indicate the calculated results of $\bar{U}$ and k on the cross sections of $x/D=10$ and 30, corresponding to the experimental ones shown in Figs. 2 (a) and (b). It is found from Fig. 11 (a) that the new term greatly suppresses turbulence throughout the cross section. Figure 11 (b) indicates that k is larger in the central region and smaller in the

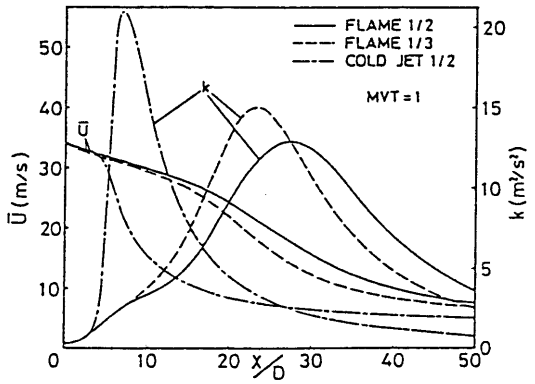

Fig. 8 Calculated axial profiles of velocity and turbulent kinetic energy along symmetry axis

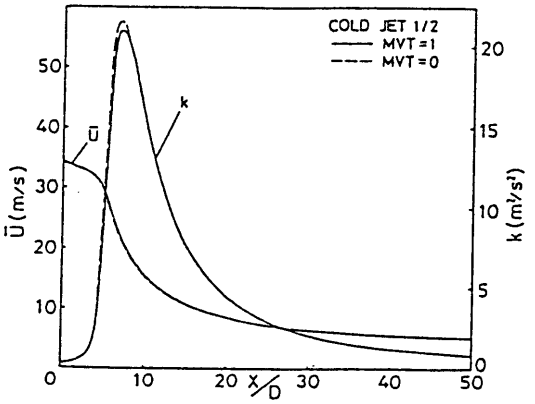

Fig. 9 Calculated axial profiles of velocity and turbulent kinetic energy along symmetry axis for Cold Jet 1/2

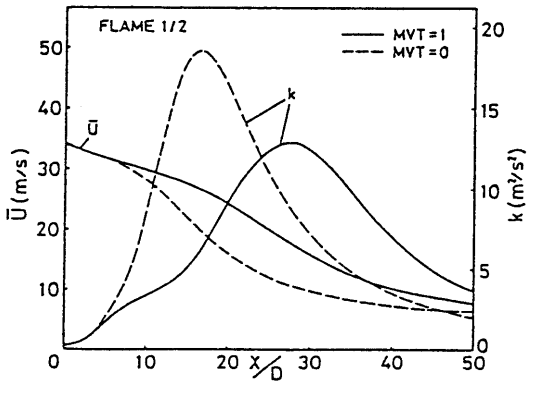

Fig. 10 Calculated axial profiles of velocity and turbulent kinetic energy along symmetry axis for Flame 1/2

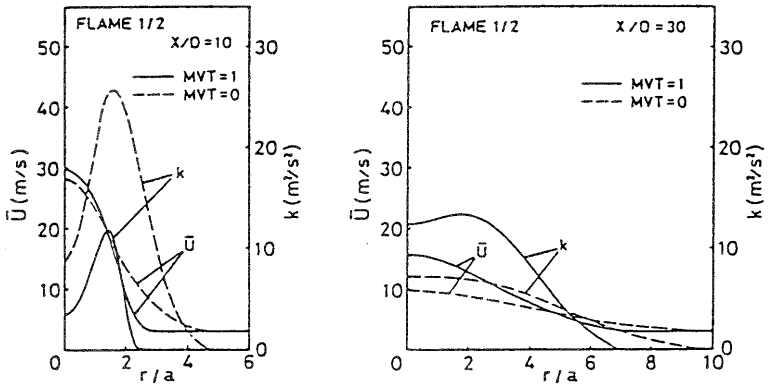

(a) The cross section of $x/D=10$ (b) The cross section of $x/D=30$

Fig. 11 Calculated radial profiles of velocity and turbulent kinetic energy on cross section for Flame 1/2

periphery in the case of MVT=1 than in MVT=0, and k ceases to exist at comparatively small radial locations in MVT=1; this is due to the fact the new dissipation term has a large effect in the peripheral region of low turbulence. Such suppression of turbulence decreases the radial diffusion flux of momentum, energy, chemical species and so on. The small diffusion flux of momentum reduces the decreasing rate of the velocity along the axis of symmetry in the case of MVT=1. Generally, the flow velocity along the axis of symmetry is kept high even downstream in jet diffusion flames, as compared with noncombustion jets. Usually, this can be attributed to thermal expansion and buoyancy, but these results suggest that the suppression of momentum diffusion due to the above mechanism should be considered as one of the causes.

Figures 12 and 13 show the calculated profiles of temperature and chemical species along the axis of symmetry and on the cross sections, corresponding to the experimental results shown in Figs. 3 and 4, respectively. Figure 12 indicates that the addition of the new dissipation term shifts to the downstream the peaks of temperature and H_2O concentration and delays the progress of combustion. This may be due to the fact that the effect of molecular viscosity changes the turbulence field, which in turn influences diffusion flux and reaction rate. It is seen in Figs. 13 (a) and (b) that all the values have narrow radial distributions in MVT=1 and wide distributions in MVT=0. This is attributed to the decrease of radial diffusion flux which is due to the suppression of turbulence in the peripheral regions caused by the new dissipation term.

It may be concluded from the comparison of the calculated results (Figs. 8~13) with the experimental

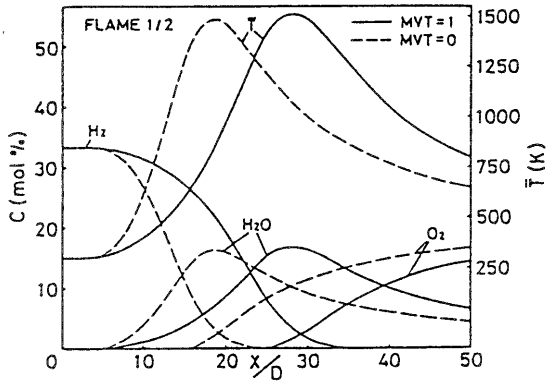

Fig. 12 Calculated axial profiles of temperature and concentrations along symmetry axis for Flame 1/2

ones (Figs. 1~4) that the consideration of the direct influence of molecular viscosity brings about a large change on the calculated results for jet diffusion flames and greatly improves the simulation.

4. Conclusions

It was beleived that the increase of molecular viscosity due to high temperature raises the dissipation rate of turbulence in low-turbulence regions in a combustion field. To verify this both experimentally and theoretically, experiments were carried out on jet diffusion flames of hydrogen, and then a numerical simulation was conducted on the experimental results. The conclusions are as follows.

(1) The present experiment confirmed that turbulence is suppressed in high-temperature and low turbulence regions situated around a nozzle exit in jet diffusion flames. In sufficiently turbulent regions, however, the dissipation rate of turbulence appeared not

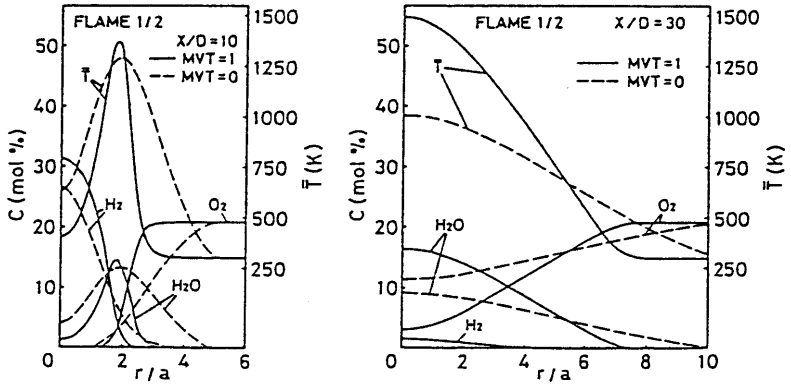

(a) The cross section of $x/D=10$ (b) The cross section of $x/D=30$

Fig. 13 Calculated radial profiles of temperature and concentrations on cross section for Flame 1/2

to be influenced by molecular viscosity even when temperature rose with combustion.

(2) A numerical calculation was conducted using a modified k-ε model with a new dissipation term of molecular viscosity. The simulation was improved greatly by using this model, and the calculated results agreed well with the experimental ones.

(3) The new term of turbulence dissipation was decided by referring to the turbulence model proposed by Jones and Launder. The effects of this term were as follows.

a) Little effect was observed on the calculated results for a non-combustion jet.

b) In flames, turbulence was suppressed greatly in high-temperature and low-turbulence regions situated around the nozzle exit and the periphery of jets.

c) The radial diffusion of various quantities in combustion fields were also suppressed due to the reduction of turbulence in the periphery.

d) Eventually, the new term largely changes the calculated results throughout the flame, because the change of turbulence distribution influences diffusion flux and reaction rate.

The present work suggested that the consideration of the direct influence of molecular viscosity is important in the modeling of jet diffusion flames. This may be also a matter of technological importance , because high temperature and low turbulence regions are supposed to exist also in practical combustors. The turbulence model proposed in the present study is merely the first step to understand the effect of molecular viscosity. Further studies must be developed to obtain the better turbulence model.

Acknowledgments

This work was supported by the grants in aid for scientific research from the Ministry of Education in Japan and for thermal engineering from the Tanigawa Foundation.

References

(1) Jones, W. P. and Launder, B. E., The Prediction of Laminarization with a Two-Equation Model of Turbulence, Int. J. Heat Mass Transf., Vol. 15, No. 2 (1975), p. 301.

(2) Jones, W. P. and Launder, B. E., The Calculation of Low-Reynolds-Number Phenomena with a Two-Equation Model of Turbulence, Int. J. Heat Mass Transf., Vol. 16, No. 6 (1973), p. 1119.

(3) Hoffmann, G. H., Improved Form of the Low-Reynolds-Number k-ε Turbulence Model, Physics of Fluids, Vol. 18, No. 3 (1975), p. 309.

(4) Kawamura, H., Trans. Jpn. Soc. Mech. Eng., (in Japanese), Vol. 45, No. 395, B (1979), p. 1038.

(5) Chien, K.-Y., Predictions of Channel and Boundary-Layer Flows with a Low-Reynolds-Number Turbulence Model, AIAA Journal., Vol. 20, No. 1 (1982), p. 33.

(6) Patel, V. C., Rodi, W. and Scheuerer, G., Turbulence Models for Near-Wall and Low-Reynolds-Number Flows: A Review, AIAA Journal., Vol. 23, No. 9 (1985), p. 1308.

(7) Scholefield, D. A. and Garside, J. E., The Structure and Stability of Diffusion Flows, Proc. 3 rd Symp. (Int.) Combust., (1953), p. 102.

(8) Hottel, H. C. and Hawthorne, W. R., Diffusion in Laminar Flame Jets, Proc. 3 rd Symp. (Int.) Combust., (1953), p. 254.

(9) Wohl, K., Gazley, C. and Kapp, N., Diffusion Flames, Proc. 3 rd Symp. (Int.) Combust., (1953), p. 288.

(10) Takeno, T. and Kotani, Y., An Experimental Study on the Stability of Jet Diffusion Flame, Acta Astronaut., Vol. 2, No. 1 (1975), p. 999.
(11) Takagi, T., Shin, H.-D. and Ishio, A., Local Laminarization in Turbulent Diffusion Flames, Combust. Flame, Vol. 37, No. 2 (1980), p. 163.
(12) Takagi, T. and Koto, S., Trans. Jpn. Soc. Mech. Eng., (in Japanese), Vol. 48, No. 436, B (1982), p. 2609.
(13) Magnussen, B. F. and Hjertager, B. H., On Mathematical Modeling of Turbulent Combustion with Special Emphasis on Soot Formation and Combustion, Proc. 16 th Symp. Int. Combust., (1977), p. 719.
(14) Laufer, J., The Structure of Turbulence in Fully Developed Pipe Flow, NACA Rep. 1174 (1954).
(15) Patankar, S. V. and Spalding, D. B., Heat and Mass Transfer in Boundary Layers, (2 nd ed.,) (1970), International Textbook Co.